Variation in Flooding Tolerance in *Populus deltoides* 'D-124' and *P. trichocarpa* x *P. deltoides* Hybrid '52-225'

Tao Yao[1,2†], Abigail Ortega-Corretjer[2,3†], Xinji Zhang[1,2], Nancy L. Engle[1,2], Kelsey R. Carter[4], Amith Reddy[1,2,6], Jun Hyung Lee[1,5], Jacob Weston[3], David J. Weston[1], Timothy J. Tschaplinski[1,2], Gerald A. Tuskan[1,2], Miaomiao Li[1,2], Jin-Gui Chen[1,2*]

[1] Biosciences Division, Oak Ridge National Laboratory, Oak Ridge, TN 37831, USA

[2] Center for Bioenergy Innovation, Oak Ridge National Laboratory, Oak Ridge, TN 37831, USA

[3] College of Arts and Sciences, University of Tennessee, Knoxville, TN 37996, USA

[4] Environmental Sciences Division, Oak Ridge National Laboratory, Oak Ridge, TN 37831, USA

[5] Department of Environmental Biology, State University of New York College of Environmental Science and Forestry, Syracuse, NY 13210, USA

[6]Department of Biology, School of Natural Sciences and Mathematics, Claflin University, Orangeburg, SC 29115, USA

* Authors for correspondence:

Jin-Gui Chen

Email: chenj@ornl.gov

† These authors have contributed equally to this work.

Summary

- Flooding poses a substantial challenge to plant survival and productivity, particularly in riparian genus like *Populus*.
- This study examines the physiological, morphological, metabolic, and molecular responses of *Populus deltoides* 'D-124' and *P. trichocarpa* x *P. deltoides* hybrid clone '52-225' under control and inundated conditions to identify differences in flooding tolerance.
- Under flooding conditions, physiological and cellular stress was more pronounced in *P. deltoides* 'D-124' than in the hybrid clone '52-225,' as evidenced by lower transpiration (E), photosynthesis (A), and chlorophyll content. In contrast, '52-225' showed reduced ROS accumulation suggesting better cellular function under stress. Morphologically, '52-225' produced more shoot-born roots, which likely enhances oxygen transport and metabolic activity during flooding. Metabolite profiling revealed both overlapping and distinct patterns of sugar and amino acid accumulation between genotypes. Gene expression analysis revealed that flooding-responsive genes, including *ADH1* and *HRE2*, were activated in both genotypes, with a more pronounced response noted in '52-225.'
- These findings extend our understanding of flooding tolerance mechanisms in *Populus* by connecting physiological traits, stress responses, and genetic regulation. This research contributes to the development of more flooding-resilient poplar varieties, with potential applications in breeding and restoration programs for flooding-prone environments.

Keywords: Flooding stress, shoot-born adventitious roots, physiological responses, metabolite profiling, *Populus deltoides*, *Populus trichocarpa* x *P. deltoides*

Introduction

Flooding is one of the most common abiotic stressors affecting plant growth and productivity, particularly in riparian and low-lying ecosystems, where fluctuating water levels frequently leads to inundation (Loreti et al. 2016). Flooding imposes substantial challenges to plants, disrupting root oxygen availability and altering physiological and metabolic processes, ultimately impacting overall plant health and survival (Pechanova et al. 2010). *Populus* species, known for their ecological and economic significance, are ideal models for studying flooding tolerance due to their rapid growth, genetic variability, and adaptability to diverse environments. Understanding the mechanisms underlying flooding tolerance in *Populus* is critical for improving resilience in forestry and bioenergy crops (Marron et al. 2015, Du et al. 2017).

The adaptive responses of plants to inundation involve complex physiological, morphological, metabolic, and molecular mechanisms. Physiologically, flooding disrupts gas exchange, photosynthetic activity, and water uptake, leading to reduced growth and biomass accumulation. Morphologically, plants often develop traits such as adventitious roots, hypertrophied lenticels, and aerenchyma to improve oxygen transport and survival in hypoxic conditions (Du et al.

2017). Metabolic adjustments incorporate the biosynthesis and transport of sugars, amino acids, and fermentation products (Kreuzwieser et al. 2009). At the molecular level, key pathways including glycolysis, fermentation, and antioxidant defense systems are activated to mitigate stress-induced damage (Xie et al. 2022). For instance, the regulation of stress-responsive genes, such as those encoding plant cysteine oxidases (PCOs) and ethylene-responsive factors (ERFs), play a crucial role in enhancing flooding tolerance (Du et al. 2017, Weits et al. 2014).

Previous studies have highlighted the significance of both physiological and molecular adaptations to plant flooding tolerance. For example, *Populus deltoides* has demonstrated the ability to alter leaf traits during post-flooding recovery, compensating for carbon fixation losses through increasing water-use efficiency rather than enhancing photosynthetic activity (Marron et al. 2015). Intraspecific progeny of *P. deltoides* vary in flooding tolerance which is associated with plant growth and rooting ability (Rodriguez et al. 2020, 2021). Machine learning approaches have been used to predict waterlogging resistance in 20 different poplar varieties, integrating physiological and environmental parameters and identifying key traits associated with inundation tolerance (Xie et al. 2022). Collectively, these studies provided a foundation for exploring interspecific and intraspecific strategies to improve flooding resilience.

In this study, we investigate the physiological, morphological, and molecular responses of *P. deltoides* 'D-124' and *P. trichocarpa* x *P. deltoides* hybrid clone '52-225' to flooding stress. These genotypes were selected based on their contrasting growth and survival characteristics under waterlogged conditions, offering a unique opportunity to dissect the mechanisms driving flooding tolerance (Drost et al. 2010). Specifically, we examined differences in gas exchange, photosynthetic efficiency, chlorophyll content, reactive oxygen species (ROS) accumulation, morphological adaptations such as shoot-born adventitious root formation, the expression of key flooding-responsive genes, and the accumulation of flooding-related metabolites. By integrating physiological, morphological, metabolic, and molecular analyses, this work expands our understanding of genotype-specific responses and their implications for flooding resilience in *Populus*.

Materials and Methods

Plant growth conditions and flooding treatment

Two genotypes of *Populus*, *P. deltoides* 'D-124' and *P. trichocarpa* x *P. deltoides* hybrid '52-225,' were used for this study. These genotypes were propagated and grown in a greenhouse at Oak Ridge National Laboratory (Oak Ridge, TN) at 25°C and a 16 h/8 h light/dark photoperiod.

Flooding conditions were simulated using a sterilized cooler where two-month-old poplar plants were partially submerged under water supplemented with 20-10-20 N-P-K fertilizer solution with water levels maintained at approximately 13 cm above the top of the pots. The water was refreshed daily to prevent stagnation and nutrient depletion.

Physiological measurement

Physiological differences in flooding tolerance were determined using a portable photosynthesis infrared gas analyzer with 6 cm^2 fluorometer attachment (LI6800F, LICOR Biosciences, Lincoln, NE, USA). Leaf-level CO_2 assimilation, stomatal conductance, PSII efficiency, and photosynthetic electron transport were measured with a saturating light of 1500 μmol m^{-2} s^{-1} and 415 ppm CO_2 concentration. Leaf vapor pressure deficit was controlled at 1.5 kPa and leaf temperature was set to 25°C. Measurements were initially collected on the first fully expanded, healthy leaf. Subsequent measurements were collected weekly on the same leaf.

Chlorophyll content measurement

Chlorophyll content was measured using a dimethyl sulfoxide (DMSO)-based extraction method following the protocol described by Lee et al. (2023). Specifically, fresh leaf discs were collected from designated plants and their fresh weight (FW) was recorded prior to extraction. Samples were then submerged in 2 mL of DMSO and incubated at 65℃ in the dark for 1 h to allow for complete pigment extraction. Absorbance readings were measured using a 96-well plate reader (0.1 mL per well) at specific wavelengths (665 nm and 648 nm) to determine chlorophyll *a* and *b* concentrations.

Quantification of ROS

H_2O_2 accumulation in the leaves of D-124 and 52-225 was quantified using the Amplex Red assay (Molecular Probes, Invitrogen), following the method of Suzuki et al. (2015) with modifications, as follows. Leaf tissues were flash-frozen in liquid nitrogen and ground to a fine powder. Subsequently, 500 μL of 50 mM sodium phosphate buffer (pH 7.4) containing 50 μM Amplex Red and 0.05 U mL^{-1} horseradish peroxidase was added. The homogenates were centrifuged at 12,000 × g for 12 min at 4°C and 400 μL of the supernatant were transferred to fresh tubes and incubated in the dark at room temperature for 30 min. Absorbance at ~585 nm was measured using a Qubit 4 Fluorometer with the preconfigured Amplex Red Peroxide Assay. H_2O_2 concentrations were determined using a standard curve ranging from 0 to 25 μM H_2O_2. Following absorbance measurements, tissue samples were dried in a speed vacuum concentrator at 30°C for 120 min and H_2O_2 accumulation was normalized to dry weight (μmol H_2O_2 mg^{-1} DW).

RNA extraction and qRT-PCR analysis

RNA extraction was completed using a modified protocol from the Sigma plant total RNA kit. Samples were ground to a fine powder in a Geno Grinder before RNA isolation. RNA quality and concentration were verified using spectrophotometric analysis. DNA synthesis and quantitative PCR (qPCR) were employed to measure the expression of flooding-responsive genes. Primers were designed using Primer3 software and qPCR reactions were conducted in triplicate to ensure accuracy. *PtEF1β* (Potri.009G01860) was utilized as a reference gene in qRT-PCR, and gene expression levels were calculated using the $2^{-\Delta\Delta CT}$ method. The primers employed for qPCR are listed in Table S1.

Metabolite determination by Gas Chromatography-Mass Spectrometry (GC-MS)

Metabolites for GC-MS analysis were extracted from ground, frozen root and leaf biomass. Approximately 150 mg root tissue was extracted twice overnight with 2.5 mL of 80% ethanol. Sorbitol (75 µL of a 1mg/mL aqueous solution) was added to the first extract as an internal standard. Following each extraction, samples were centrifuged at 3,234 x g for 20 min and the supernatants were decanted to a vial. Extracts from both days were combined, thoroughly mixed, and a 1-mL aliquot was dried under a stream of nitrogen for further derivatization and analysis. The dried extract was dissolved in 500 µL silylation-grade acetonitrile (Thermo Scientific, TS-20062) followed by addition of 500 µL of MSTFA plus 1% TMCS (2,2,2-Trifluoro-N-methyl-N-(trimethylsilyl)-acetamide, Chlorotrimethylsilane; Thermo Scientific, TS-48915). Samples were then heated at 70°C for 1 h to generate trimethylsilyl (TMS) derivatives. Two days after derivatization, a 1 µL aliquot was analyzed using an Agilent 7890A/5975C inert XL GC-MS system. Metabolites were identified using a Wiley Registry/ NIST Mass Spectral Library 2023 in addition to a large user-created database of TMS-derivatized compounds. Metabolite peaks were extracted using selected key mass-to-charge (m/z) ions to reduce interference from co-eluting metabolites. Quantified was performed as previously described (Abraham et al. 2016), with peak areas scaled back to the total ion chromatogram using previously calculated scaling factors and normalized to internal standard recovery, extract volume analyzed, sample mass, and injection volume.

Data analysis

Statistical analyses were performed to evaluate differences between genotypes and treatments. One-way ANOVA was used to identify significant differences among groups, followed by Tukey's HSD post-hoc test to compare individual means. A significance threshold of $P \leq 0.05$ was applied. Bar plots were generated using either Origin software or the ggplot2 package in R to visualize group differences.

Results

To assess the flooding tolerance of different *Populus* genotypes, we selected 2-month-old of *P. deltoides* D-124 and *P. trichocarpa* x *P. deltoides* hybrid 52-225 and conducted the flooding treatment with partial submerging of the stems. After 28 days of inundation, D-124 plants showed leaf yellowing and senescence, while 52-225 plants maintained green leaves (Figure 1a). Consistently, flooding significantly reduced leaf and stem biomass in D-124, but not in 52-225 (Figure 1b and c). Over the course of one month of flooding treatment, the relative growth rate of D-124 was reduced below that of 52-225 (50% and 70% of plant height, respectively) (Figure 1d). Across all measured parameters, *P. trichocarpa* x *P. deltoides* 52-225 plants were more flooding tolerant than *P. deltoides* D-124 plants.

Whole-plant and physiological adjustments

Flooding-tolerant trees tend to develop adventitious roots on stems to compensate for the below-ground root damage caused by low oxygen. We observed the shoot-born formation of adventitious roots after two weeks of flooding treatment on 52-225 plants; however, no shoot-born roots were formed on the stems of D-124 plants within the one-month flooding treatment (Figure 2). Shoot-born root formation was one of the first morphological adaptation mechanisms that contributed to a genotype-specific flooding tolerance.

Under prolonged flooding treatment, we examined plant gas exchange and chlorophyll fluorescence in two different *Populus* genotypes. The LiCor 6800-based measurements indicated a dramatic inhibition of gas exchange and CO_2 fixation in *P. deltoides* D-124 leaves. However, net photosynthesis and stomatal conductance were less affected in 52-225 leaves, likely contributing to enhanced shoot growth and survival under flooding conditions. Photosystem II efficiency and electron transport rate (ETR) were also compared between D-124 and 52-225 leaves. Although both genotypes exhibited reduced PSII efficiency and photosynthetic ETR under hypoxic conditions, 52-225 maintained significantly higher chlorophyll fluorescence and ETR than D-124. Overall, *P. trichocarpa* x *P. deltoides* hybrid 52-225 plants experienced fewer detrimental physiological adjustments than *P. deltoides* D-124 plants under flooding treatment.

To further investigate photosynthetic damage caused by flooding, we examined the chlorophyll content of both genotypes with or without flooding treatment. Flooding treatment significantly reduced chlorophyll content of *P. deltoides* D-124 plants in either total chlorophyll, chlorophyll *a*, or chlorophyll *b*. However, flooding only marginally changed chlorophyll contents in 52-225 plants (Figure 4). This difference led to chlorosis and impaired photosynthetic efficiency in D-124 plants, whereas 52-225 plants were less chlorotic.

Metabolic and oxidative changes

To investigate the metabolic adaptations of D-124 and 52-225 in response to flooding, GC-MS was used to quantify the metabolite abundance of sugars, amino acids and secondary metabolites in roots. One of the fermentation products, lactic acid, a byproduct of ATP biosynthesis, significantly increased in both genotypes, yet 52-225 accumulated more than that in D-124, indicating higher ability for ATP production in 52-225 roots under hypoxic conditions. We also observed an increase of sucrose and arabinose in flooded 52-225 plants, while only sucrose content was increased in flood-treated D-124 roots (Figure 5a and b).

The concentrations of several amino acids, including 5-oxo-proline, alanine, GABA, and glycine were significant increased in D-124 roots, whereas alanine, GABA, glutamine, and glycine showed significant increases in 52-225 roots in response to flooding. Phenylalanine abundance decreased in both D-124 and 52-225 roots, while asparagine, leucine, and isoleucine only decreased in 52-225. The overall shifts in fermentation associated metabolites, carbohydrates, and amino acids suggest a stronger flooding response in 52-225 plants (Figure 5c).

Oxidative stress is one of the factors that cause damage to membrane integrity in plant cells leading to chlorophyll breakdown and photosynthetic disruption. To assess the ROS accumulation in D-124 and 52-225, we quantified the leaf H_2O_2 content following the flooding treatment. The results revealed that H_2O_2 accumulation was three-fold higher in D-124 compared to 52-225 plants (Figure 6), suggesting that 52-225 plants are either more capable of inhibiting ROS production or more efficient at ROS detoxification under flooding conditions.

Enhanced hypoxia signaling

To investigate the molecular mechanisms of different flood tolerance capabilities between D-124 and 52-225, we compared the expression of hypoxia signaling genes in these two genotypes. Alcohol dehydrogenase 1 (ADH1) has been reported to enhance plant flooding tolerance (Xuan et al., 2021) and we observed that two of the *ADH1* genes were highly induced in 52-225 plants under flooding conditions, whereas their induction was much lower in flooded D-124 plants. The expression of *ADH1* is regulated by ethylene response factor (ERF) VII transcription factors, which activates hypoxia signaling and flooding tolerance (Giuntoli and Perata, 2018). Consistently, we also observed enhanced gene expression of *PCO2* in hypoxia signaling in flooded 52-225 plants relative to that in flooded D-124 plants. Furthermore, one of the hypoxia-responsive ERFs, *HRE2,* was highly expressed in both control and flooding-treated 52-225 plants compared to D-124 plants under same conditions (Weits et al. 2014, Figure 7). These findings suggest that 52-225 plants may be primed for hypoxia signaling and more responsive to flooding stress via elevated *HRE2* expression.

Discussion

In this study, we compared the morphological, physiological, and molecular changes between the *P. deltoides* D-124 and the *P. trichocarpa* x *P. deltoides* hybrid 52-225 in response to flooding treatment. Compared to the flooding susceptible genotype D-124, the flooding tolerance of poplar 52-225 adopted multiple strategies to cope with hypoxia stress (Figure 8), including the formation of adventitious roots and enhanced respiration rate. The reduction of ROS production in 52-225 potentially also leads to less damage to the membrane system. All these developmental and physiological changes are likely driven by the up regulation of flooding tolerance genes such as *ADH1* and *HRE2*.

Although the D-124 trees exhibited lower flooding tolerance than the 52-225 trees, they still demonstrated molecular and metabolic responses to flooding stress. This is consistent with previous findings that *P. deltoides* is tolerant to winter flooding (Miao et al., 2017). In D-124 roots, we observed a significant increase in the expression of *ADH1* and *HRE2*, which was associated with elevated lactic acid accumulation (Figure 7). Enhanced carbohydrate accumulation supports the glycolysis–fermentation pathway for ATP production and is a known mechanism of flooding stress tolerance (Bailey-Serres and Voesenek 2008). Similarly, sucrose and several amino acids accumulated in the roots of flooding-treated D-124 plants (Figure 5). Alanine accumulation has been reported to serve as the indicator for hypoxia stress, whereas GABA shunt is known to

alleviate the deleterious flooding effects (Jaeger et al. 2009; Lu et al. 2024). These metabolic changes were reported to promote stress adaptation to hypoxia (Kreuzwieser et al. 2009). However, D-124 trees did not form shoot-borne roots and showed a more severe impairment in photosynthetic adjustment, leading to flooding-sensitive symptoms such as leaf senescence and abscission.

The tree genus *Populus* comprises approximately 32 species. Upland poplars, such as *P. tremuloides*, are relatively drought-tolerant, while black cottonwoods, such as *P. trichocarpa*, are pioneering and dominant trees in riparian zones, which typically experience flooding (Rood et al. 2010; Rodriguez et al. 2020). Though in general, *P. deltoides* has been shown to be more drought-tolerant than *P. trichocarpa*and hybrid *P. trichocarpa* x *P. deltoides* hybrids (Tschaplinski et al. 2006), but the hybrid performs better under flooding conditions (Street et al. 2006, Figure 1). This may be due, in part, to the greater ease of adventitious rooting in *P. trichocarpa* x *P. deltoides* hybrids versus *P. deltoides* genotypes (Heilman et al, 1994). Given the variability in flooding tolerance between species and genotypes, our data suggests that interspecific or intraspecific hybrids can be developed that display enhanced flooding tolerance. In addition, given that we observed drastic differences in flooding-related phenotypic traits between 52-225 and D-124, our findings also suggest that the pseudobackcross progeny family '52-124', generated from the cross between 52-225 and D-124 trees, may serve as excellent resource for genetic mapping efforts to identify flooding tolerance genes as well as selecting flooding tolerant germplasm for tree breeding programs (Drost et al. 2010). In addition, further research is merited on the role of *HRE2* in flood tolerance using transgenic approaches.

Acknowledgements

This material is based upon work supported by the Center for Bioenergy Innovation (CBI), U.S. Department of Energy, Office of Science, Biological and Environmental Research Program under Award Number ERKP886. This research was also in part supported by Oak Ridge National Laboratory Research Student Internships Program, sponsored by the U.S. Department of Energy and administered by the Oak Ridge Institute for Science and Education.

Authors' contributions

T.Y. and J.-G.C. conceived and designed the project; T.Y., A.O.-C., X.Z., N.L.E., K.R.C., A.D., J.H.L., J.W., T.J.T, and M.L. performed sample preparation, laboratory analyses and data analyses; T.Y., A.O.-C., and J.-G.C. wrote the manuscript with contributions from D.J.W, T.J.T, and G.A.T. and all authors critically reviewed and approved the manuscript. T.Y. and A.O.-C. contributed equally to this work.

Supplementary data

Table S1. List of used primers in qRT-PCR.

Conflict of interest

None declared.

Funding

This study was funded by the Center for Bioenergy Innovation (CBI), U.S. Department of Energy, Office of Science, Biological and Environmental Research Program under Award Number ERKP886.

Data availability

The metabolomics data will be publicly available through the DOE Office of Scientific and Technical Information.

Reference

Abraham, P.E., Yin, H., Borland, A.M., Weighill, D., Lim, S.D., De Paoli, H.C., Engle, N., Jones, P.C., Agh, R., Weston, D.J., Wullschleger, S.D., Tschaplinski, T., Jacobson, D., Cushman, J.C., Hettich, R.L., Tuskan, G.A. and Yang, X. (2016) Transcript, protein and metabolite temporal dynamics in the CAM plant Agave. Nature Plants, 2, 16178.

Bailey-Serres, J. and Voesenek, L.A.C.J. (2008) Flooding Stress: Acclimations and Genetic Diversity. Annu Rev Plant Biol, 59, 313-339.

Drost, D.R., Benedict, C.I., Berg, A., Novaes, E., Novaes, C.R., Yu, Q., Dervinis, C., Maia, J.M., Yap, J. and Miles, B. (2010) Diversification in the genetic architecture of gene expression and transcriptional networks in organ differentiation of *Populus*. Proc Natl Acad Sci U.S.A., 107, 8492-8497.

Du Z, Zhou X, Wang H, Song X, Chen Z. 2017. Understanding physiological and molecular mechanisms of *Populus deltoides* 'DanHongYang' tolerance to waterlogging by comparative transcriptome analysis. Sci Rep. 7(1):17887.

Giuntoli, B. and Perata, P. (2018) Group VII Ethylene Response Factors in Arabidopsis: Regulation and Physiological Roles. Plant Physiol, **176**, 1143-1155.

Heilman P.E., G. Ekuan, and D.B. Fogle. 1994. First-order root development from cuttings of *Populus trichocarpa* x *P. deltoides* hybrids. Tree Physiol. 14: 911-920. Jaeger, C., Gessler, A., Biller, S., Rennenberg, H. and Kreuzwieser, J. (2009) Differences in C metabolism of ash species and provenances as a consequence of root oxygen deprivation by waterlogging. J Exp Bot, 60, 4335-4345.

Kreuzwieser J, Hauberg J, Howell KA, Carroll A, Rennenberg H, Millar AH, Whelan J (2009) Differential response of gray poplar leaves and roots underpins stress adaptation during hypoxia. Plant Physiol 149: 461-473.

Lee, J.H., Burdick, L.H., Piatkowski, B., Carrell, A.A., Doktycz, M.J., Pelletier, D.A. and Weston, D.J. (2023) A rapid assay for assessing bacterial effects on Arabidopsis thermotolerance. Plant Methods, 19, 63.

Loreti E, van Veen H, Perata P. 2016. Plant responses to flooding stress. Curr Opin Plant Biol. 33:64\u201371.

Lu, Y., Zhang, S., Xiang, P., Yin, Y., Yu, C., Hua, J., Shi, Q., Chen, T., Zhou, Z., Yu, W., Creech, D.L. and Lu, Z. (2024) Integrated small RNA, transcriptome and physiological approaches provide insight into Taxodium hybrid 'Zhongshanshan' roots in acclimation to prolonged flooding. Tree Physiol, 44.

Marron N, Bastien C, Sabatti M, Taylor G, Ceulemans R. 2015. Leaf traits related to productivity during post-flooding recovery in *Populus deltoides*. Trees 29(5):1525\u20131537.

Miao LF, Yang F, Han CY, Pu YJ, Ding Y, Zhang LJ (2017) Sex-specific responses to winter flooding, spring waterlogging and post-flooding recovery in *Populus deltoides*. Sci Rep 7: 2534.

Rodríguez, M.E., Lauff, D., Cortizo, S. and Luquez, V.M. (2020) Variability in flooding tolerance, growth and leaf traits in a *Populus deltoides* intraspecific progeny. Tree Physiol, 40, 19-29.

Rodríguez, M.E., Mozo, I., Cortizo, S., Cappa, E.P. and Luquez, V.M. (2021) Early rooting and flooding tolerance in cuttings from a *Populus deltoides* full-sib family under greenhouse conditions. Can J For Res, 51, 732-741.

Rood, S.B., Nielsen, J.L., Shenton, L., Gill, K.M. and Letts, M.G. (2010) Effects of flooding on leaf development, transpiration, and photosynthesis in narrowleaf cottonwood, a willow-like poplar. Photosynth Res, 104, 31-39.

Street, N.R., Skogström, O., Sjödin, A., Tucker, J., Rodríguez-Acosta, M., Nilsson, P., Jansson, S. and Taylor, G. (2006) The genetics and genomics of the drought response in *Populus*. Plant J, 48, 321-341.

Suzuki, N., Devireddy, A.R., Inupakutika, M.A., Baxter, A., Miller, G., Song, L., Shulaev, E., Azad, R.K., Shulaev, V. and Mittler, R. (2015) Ultra-fast alterations in mRNA levels uncover multiple players in light stress acclimation in plants. Plant J: For Cell and Molecular Biology, 84, 760-772.

Tschaplinski, T., G.A. Tuskan, M.M. Sewell, G.M. Gebre, D.E. Todd and C.D. Pendley. 2006. Phenotypic variation and QTL identification for osmotic potential in an interspecific hybrid inbred F2 poplar pedigree growing under contrasting environments. Tree Physiol. 26:595-604.

Weits, D.A., Giuntoli, B., Kosmacz, M., Parlanti, S., Hubberten, H.-M., Riegler, H., Hoefgen, R., Perata, P., van Dongen, J.T. and Licausi, F. (2014) Plant cysteine oxidases control the oxygen-dependent branch of the N-end-rule pathway. Nat Commun, 5, 3425.

Xie X, Zhang X, Shen J, Du K. 2022. Poplar waterlogging resistance: modeling and evaluating. Front Plant Sci. 13:821365.

Xuan, L., Hua, J., Zhang, F., Wang, Z., Pei, X., Yang, Y., Yin, Y. and Creech, D.L. (2021) Identification and Functional Analysis of ThADH1 and ThADH4 Genes Involved in Tolerance to Waterlogging Stress in Taxodium hybrid 'Zhongshanshan 406'. Genes, 12.

FIGURES

Figure 1. Plant growth of *Populus deltoides* 'D-124' and *P. trichocarpa* x *P. deltoides* '52-225' under control or flooding conditions.

Figure 2. Shoot-born root formation in *Populus deltoides* 'D-124' and *P. trichocarpa* x *P. deltoides* '52-225' under control or flooding conditions.

Figure 3. Photosynthetic performance of *Populus deltoides* 'D-124' and *P. trichocarpa* x *P. deltoides* '52-225' under control or flooding conditions.

Figure 4. Leaf chlorophyll content and electrolyte leakage of *Populus deltoides* 'D-124' and *P. trichocarpa* x *P. deltoides* '52-225' under control or flooding conditions.

Figure 5. Metabolic profiling in roots of *Populus deltoides* 'D-124' and *P. trichocarpa* x *P. deltoides* '52-225' under control or flooding conditions.

Figure 6. H_2O_2 accumulation in *Populus deltoides* 'D-124' and *P. trichocarpa* x *P. deltoides* '52-225' under control or flooding conditions.

Figure 7. Expression of flooding tolerant genes in *Populus deltoides* 'D-124' and *P. trichocarpa* x *P. deltoides* '52-225' under control or flooding conditions.

Figure 8. Working model of different adaptation mechanisms to flooding in *Populus*.

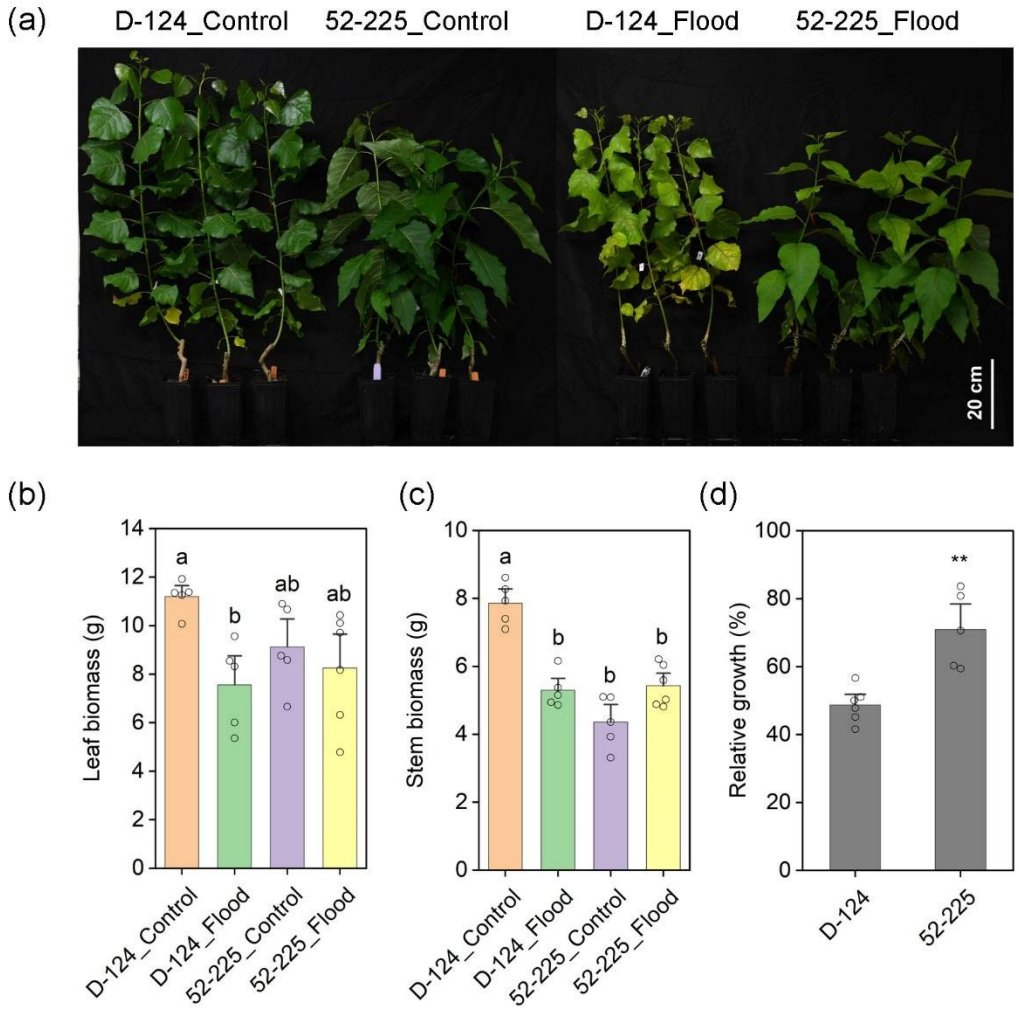

Figure 1. Plant growth of *Populus deltoides* 'D-124' and *P. trichocarpa* x *P. deltoides* '52-225' under control or flooding conditions. (**a**) Representative images of plants showing overall growth under control and flooding conditions for both genotypes. (**b**) Leaf biomass (g), (**c**) stem biomass (g), and (**d**) relative plant growth (%) due to flooding for 'D-124' and '52-225' genotypes. Bars represent mean±SE (n≥5). Different letters above the bars indicate statistically significant differences ($P \leq 0.05$).

Figure 2. Shoot-born root formation in *Populus deltoides* 'D-124' and *P. trichocarpa* x *P. deltoides* '52-225' under control or flooding conditions. Representative image shows the formation of shoot-born roots in both genotypes. Flooded plants of genotype 52-225 exhibited significant development of shoot-born roots, whereas minimal or no root formation was observed in D-124 under flooding conditions. Scale bar=20 cm.

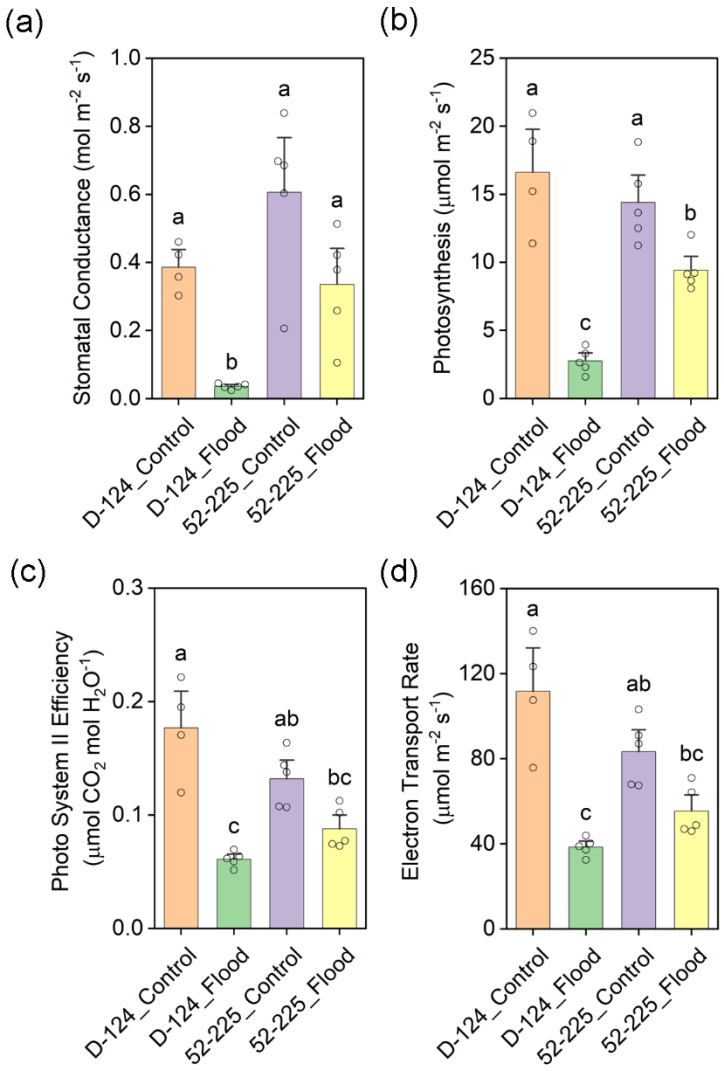

Figure 3. Photosynthetic performance of *Populus deltoides* 'D-124' and *P. trichocarpa* x *P. deltoides* '52-225' under control or flooding conditions. (**a**) Stomatal conductance (mol m^{-2} s^{-1}), (**b**) Photosynthetic rate (µmol m^{-2} s^{-1}), (**c**) Photo System II Efficiency (µmol CO_2 mol H_2O^{-1}), and (**d**) Electron Transport Rate (µmol m^{-2} s^{-1}) were measured for both genotypes. Bars represent mean±SE ($n \geq 5$). Different letters above the bars indicate statistically significant differences among treatments and genotypes ($P \leq 0.05$).

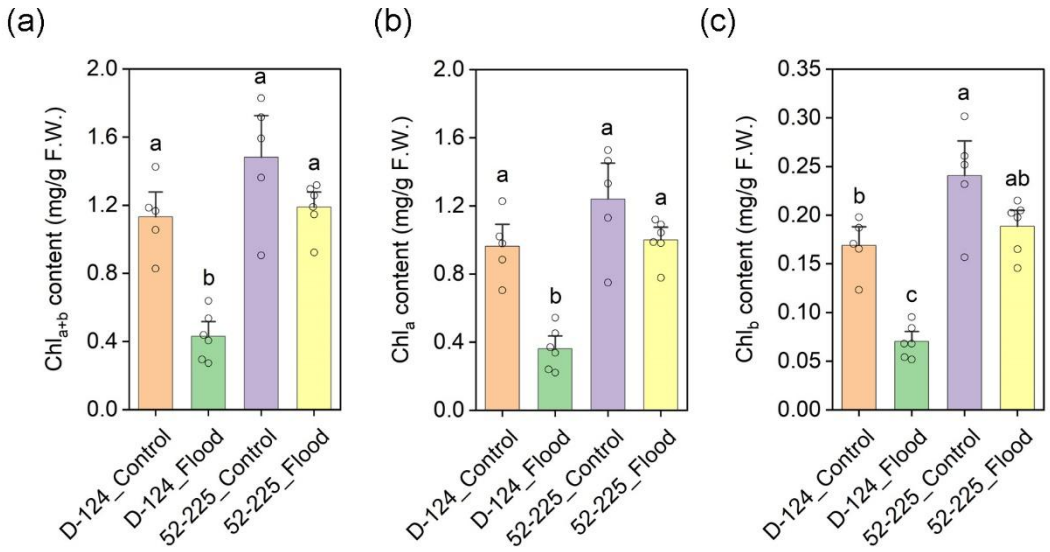

Figure 4. Leaf chlorophyll content and electrolyte leakage in *Populus deltoides* 'D-124' and *P. trichocarpa* x *P. deltoides* '52-225' under control or flooding conditions. (**a**) Total chlorophyll content (Chl *a*+*b*), (**b**) chlorophyll *a* content (Chl *a*), and (**c**) chlorophyll *b* content (Chl *b*) measured in fresh weight (mg/g FW). Bars represent mean±SE (n≥5). Different letters above the bars indicate statistically significant differences ($P \leq 0.05$).

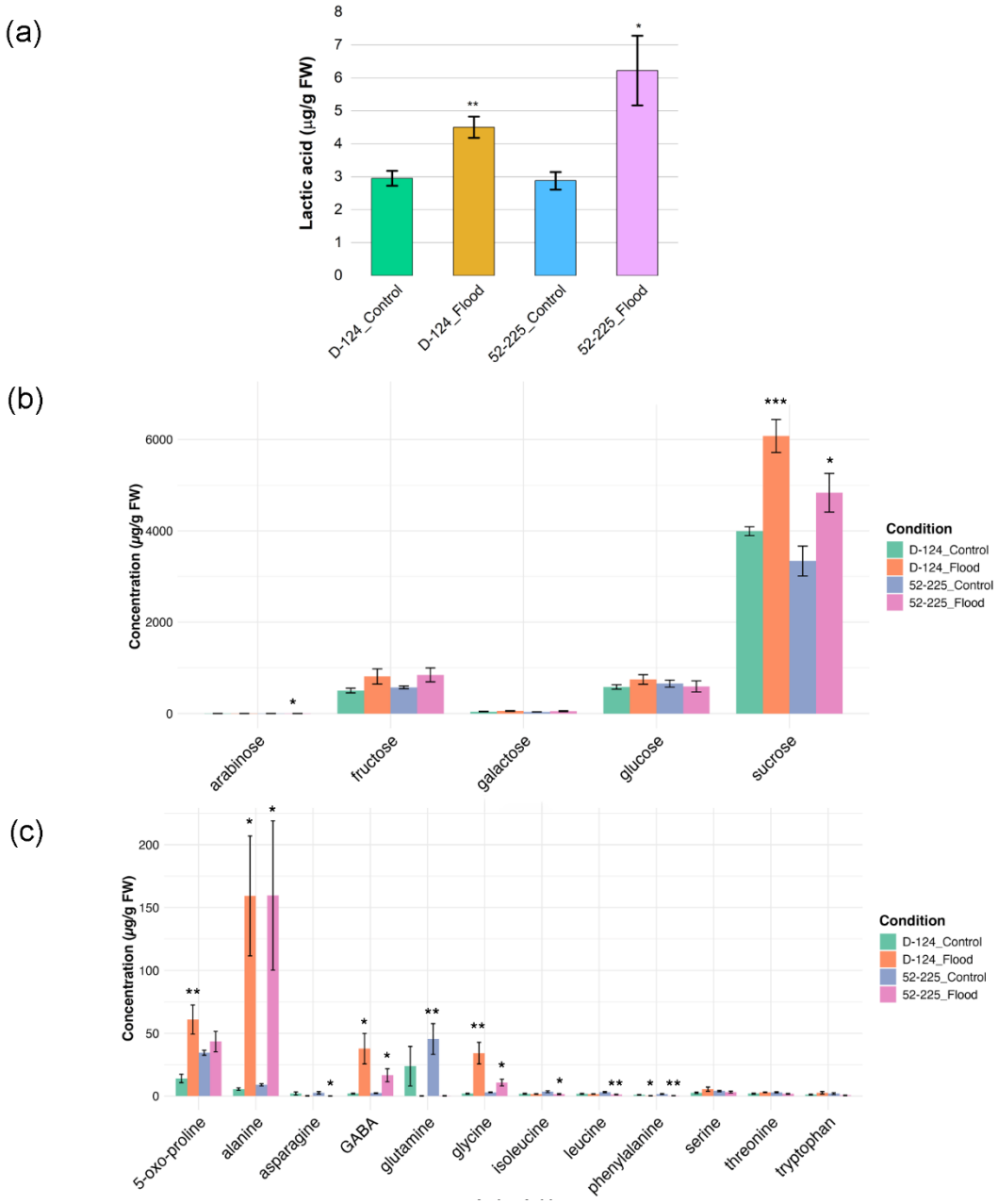

Figure 5. Metabolic profiling of roots of *Populus deltoides* 'D-124' and *P. trichocarpa* x *P. deltoides* '52-225' under control or flooding conditions. Accumulation of lactic acid (**a**), Carbohydrate (**b**), and amino acids (**c**) in the roots of *P. deltoides* 'D-124' and *P. trichocarpa* x *P. deltoides* '52-225' under control or flooding conditions are presented. Bars represent the mean±SE ($n \geq 5$). Asterisks indicate statistically significant differences between control and flood conditions ($^{*}P \leq 0.05$; $^{**}P \leq 0.01$; $^{***}P \leq 0.001$).

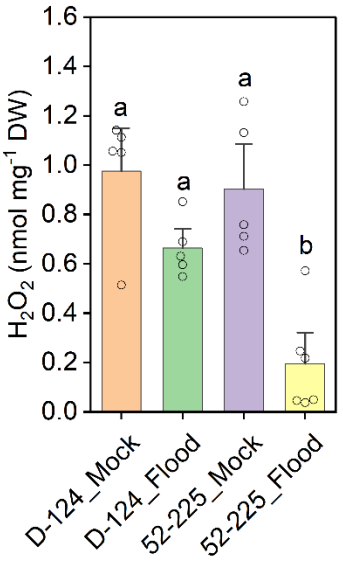

Figure 6. H_2O_2 accumulation in *Populus deltoides* 'D-124' and *P. trichocarpa* x *P. deltoides* '52-225' under flooding conditions. Bars represent the mean±SE ($n \geq 5$). Different letters above the bars indicate statistically significant differences ($P \leq 0.05$).

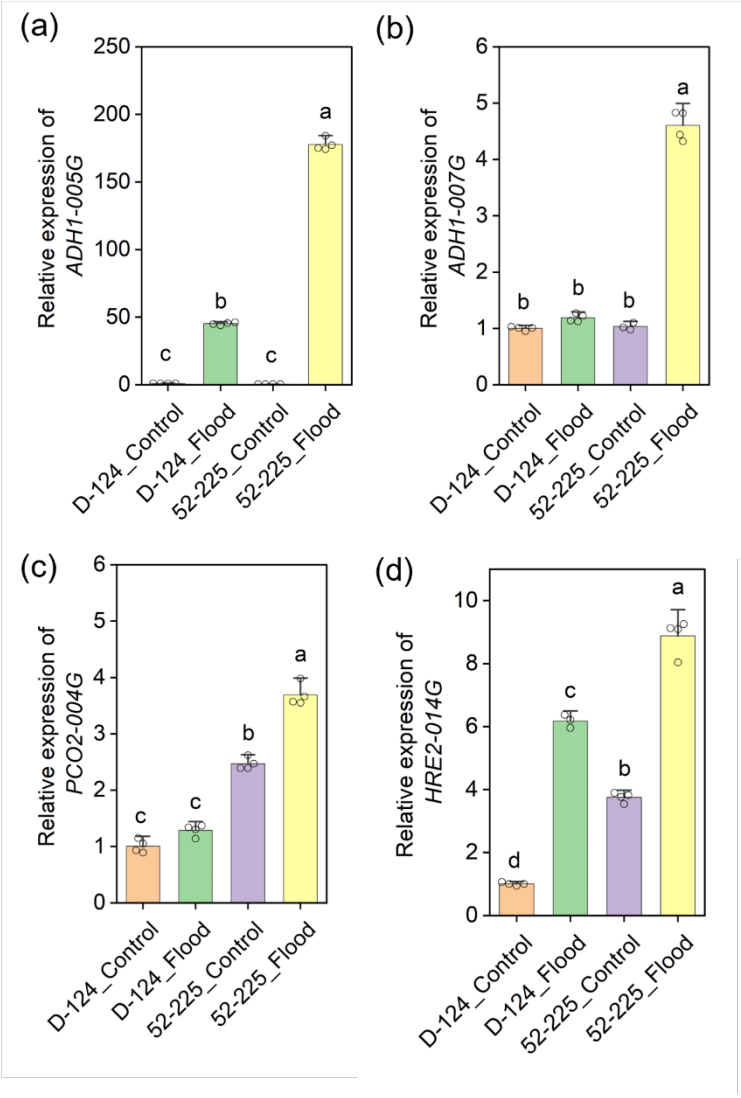

Figure 7. Expression of flooding tolerant genes in *Populus deltoides* 'D-124' and *P. trichocarpa* x *P. deltoides* '52-225' under control or flooding conditions. (**a**–**d**) Quantitative real-time (qRT)-PCR analysis of expression levels of *ADH1-005G* (a), *ADH1-007G* (b), *PCO2-004G* (c), and *HRE2-014G* (**d**) in the roots of *P. deltoides* 'D-124' and *P. trichocarpa* x *P. deltoides* '52-225' under control or flood conditions. Total RNA from control and flooded *Populus* roots was used for qRT-PCR analysis. Error bars indicate ± SD (n≥5 independent plants). Different letters indicate statistically significant among four groups as analyzed by one-way ANOVA followed by Tukey's test ($P \leq 0.05$).

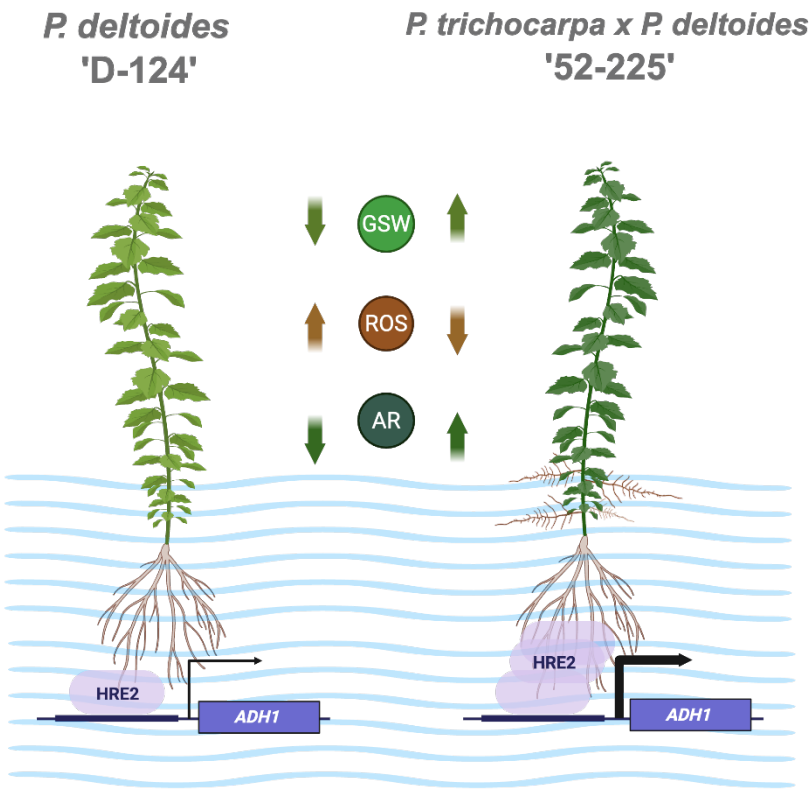

Figure 8. Working model of different adaptation mechanisms to flooding in *Populus*. Schematic illustration shows morphological, physiological and metabolic responses of the two genotypes under flooding conditions. Genotype '52-225' demonstrates increased stomatal conductance (GSW) and enhanced adventitious root (AR) formation while maintaining lower reactive oxygen species (ROS) accumulation. In contrast, genotype 'D-124' exhibits decreased stomatal conductance, reduced adventitious root formation, and elevated ROS accumulation under similar conditions. Furthermore, '52-225' shows enhanced gene expression of *HRE2* and *ADH1* in hypoxia signaling compared to 'D-124'.